# Quartz enhanced photoacoustic $H_2S$ gas sensor based on a fiber-amplifier source and a custom tuning fork with large prong spacing

Hongpeng Wu,[1] Angelo Sampaolo,[2,3] Lei Dong,[1,3,a)] Pietro Patimisco,[2] Xiaoli Liu,[1] Huadan Zheng,[1] Xukun Yin,[1] Weiguang Ma,[1] Lei Zhang,[1] Wangbao Yin,[1] Vincenzo Spagnolo,[2] Suotang Jia,[1] and Frank K. Tittel[3]
[1]*State Key Laboratory of Quantum Optics and Quantum Optics Devices, Institute of Laser Spectroscopy, Shanxi University, Taiyuan 030006, China*
[2]*Dipartimento Interateneo di Fisica, Università degli Studi di Bari and Politecnico di Bari, CNR-IFN UOS BARI, Via Amendola 173, Bari 70126, Italy*
[3]*Department of Electrical and Computer Engineering, Rice University, Houston, Texas 77005, USA*

(Received 24 July 2015; accepted 3 September 2015; published online 15 September 2015)

A quartz enhanced photoacoustic spectroscopy (QEPAS) sensor, employing an erbium-doped fiber amplified laser source and a custom quartz tuning fork (QTF) with its two prongs spaced ~800 $\mu$m apart, is reported. The sensor employs an acoustic micro-resonator (AmR) which is assembled in an "on-beam" QEPAS configuration. Both length and vertical position of the AmR are optimized in terms of signal-to-noise ratio, significantly improving the QEPAS detection sensitivity by a factor of ~40, compared to the case of a sensor using a bare custom QTF. The fiber-amplifier-enhanced QEPAS sensor is applied to $H_2S$ trace gas detection, reaching a sensitivity of ~890 ppb at 1 s integration time, similar to those obtained with a power-enhanced QEPAS sensor equipped with a standard QTF, but with the advantages of easy optical alignment, simple installation, and long-term stability.
 [http://dx.doi.org/10.1063/1.4930995]

Laser based trace gas detection is widely used in applications, such as environmental monitoring, industrial process control, and medical diagnostics.[1–4] Quartz enhanced photoacoustic spectroscopy (QEPAS) is a well-established sensor technique for detecting and quantifying trace gas species, in which a quartz tuning fork (QTF) is employed to detect acoustic oscillations induced in an absorbing gas by modulated optical radiation.[5,6] In a conventional QEPAS setup, an acoustic micro-resonator (AmR), formed by one or two metallic thin tubes, is usually used in an "off-beam" or "on-beam" configuration to obtain a higher detection sensitivity.[6–9] Typically, the "on-beam" configuration provides the best QEPAS signal-to-noise ratio.[6] The combination of a QTF and an AmR is usually referred to as a spectrophone. It is critical to avoid laser beam illumination of the spectrophone for both configurations, since the radiation blocked by them results in an undesirable nonzero background and hence strongly limits the sensor detection sensitivity.[10–12]

One of the fundamental features of the QEPAS technique is that the detection sensitivity of QEPAS based sensors is proportional to excitation laser power.[13–15] This makes QEPAS based sensor performance benefit from the development of the high-power semiconductor lasers or from the enhanced excitation laser power.[16] An optical fiber amplifier is an excellent choice for boosting laser power.[17,18] Its basic operating principle requires a short length optical fiber doped with a small amount of rare-earth ions, such as erbium, and a semiconductor diode as a pumping laser source. In principle, an optical fiber amplifier can achieve amplification factors of up to 3 orders of magnitude for input signals that occur within the gain bandwidth of the dopant, in a wide range of wavelengths (0.65–2 $\mu$m).[14] Benefitting from the development of the telecommunication industry, in which the laser power is boosted for delivering optical signals over long distances, robust optical fiber amplifiers operating in three telecommunication bands (1450–1550 nm, 1520–1570 nm, and 1565–1610 nm) are commercially readily available at low cost. Recently, a first demonstration of a QEPAS sensor employing a standard QTF and a fiber amplifier for sub-ppm $H_2S$ detection was reported.[12] As the gap size of standard QTF prongs is only ~0.3 mm, an AmR in an "off beam" configuration was employed to reduce the noise induced by stray light hitting the spectrophone.[8] Even so, the offset of the sensor background noise was ~17 times higher than the theoretical thermal noise value. In addition, an electrical modulation cancellation method was employed to remove this nonzero background, which, however, resulted in a complex sensor system with a poor long-term stability.

In this letter, we report the development of a fiber-amplifier-enhanced QEPAS sensor for $H_2S$ detection employing an erbium-doped fiber amplified 1582 nm distributed feedback (DFB) laser and a custom QTF having a spacing of ~800 $\mu$m between the QTF prongs. This approach combines the main benefits of conventional QEPAS technique, with the merit of using a watt-level excitation laser source, provided by a commercially available erbium-doped fiber amplifier. In addition, the employment of a custom QTF with large prong spacing allows the use of AmR in an "on-beam" configuration. As a result, the fiber-amplifier-enhanced QEPAS sensor is characterized by easy optical alignment, simple installation and long-term stability.

The custom QTF and standard QTF are schematically shown in Fig. 1. Their main geometrical parameters and electrical parameters[19] at room temperature ($T = 297.2$ K) and atmospheric pressure ($P_0 = 760$ Torr) are reported in Table I. Standard photolithographic techniques are used to

a)Electronic mail: donglei@sxu.edu.cn

 

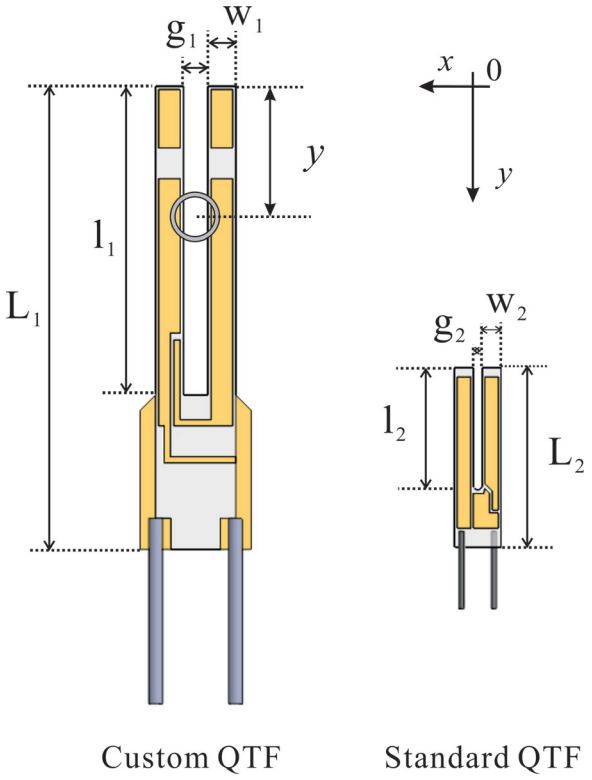


FIG. 1. Custom QTF with an "on-beam" AmR configuration and standard bare QTF with respective notation of their dimensions. The tubes were centered between the tines. *y* is the distance from the QTF opening to the center of the tubes. The proportion of their dimensions represents the actual size. Chromium/gold layers are deposited on both sides of the custom QTF providing electrical contacts similar to a standard QTF.

etch the custom QTF, starting from a z-cut quartz wafer. Chromium/gold contacts are deposited on both sides of the QTF.[20] The custom QTF has a similar geometry as the standard QTF, but is ~4.6 times larger in size. Spagnolo *et al.* have demonstrated theoretically[21] and experimentally[19,20] that the custom QTF behaves like a standard QTF transducer in terms of *Q*-factor and resonance frequency. Hence, the standard QTF can be replaced with a custom QTF in QEPAS sensing system.

A schematic of the experimental setup used to demonstrate the performance of the fiber-amplifier-enhanced QEPAS sensor with a custom tuning fork is shown in Fig. 2. Mostly due to the large prongs spacing, we were able to employ an "on-beam" QEPAS configuration to further improve the sensor detection sensitivity. A DFB laser (FITEL, Inc., Model FRL15DCWD-A82) with a wavelength of 1582.1 nm was used as the excitation source. The near-infrared, distributed

TABLE I. Dimensions and electrical parameters of a custom QTF and a standard QTF. The electrical parameters of custom QTF were measured in pure $N_2$ at atmospheric pressure ($P_0 = 760$ Torr) and room temperature ($T = 297.2$ K), while the electrical parameters of standard QTF were typical values in these conditions.

| | Geometrical parameters | | | | Electrical parameters | | |
|---|---|---|---|---|---|---|---|
| | g (μm) | L (mm) | w (mm) | L (mm) | $f_0$ (Hz) | *Q*-factor | *R*(kΩ) |
| Custom QTF | 800 | 10 | 0.9 | 15 | 7205 | 8536 | 286 |
| Standard QTF | 300 | 3.8 | 0.6 | 6 | 32 768 | 12 000 | 120 |

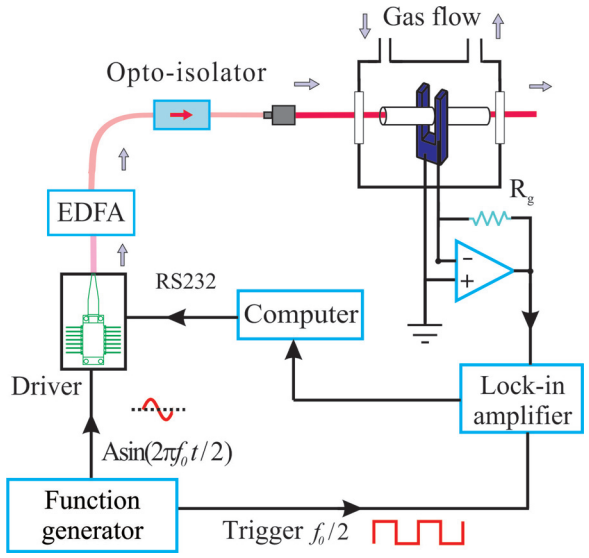


FIG. 2. Schematic of fiber-amplifier-enhanced QEPAS sensor using a custom tuning fork and an erbium-doped fiber amplifier. EDFA: Erbium-doped fiber amplifier.

feedback laser was mounted onto a driver board which was used to control the laser temperature and current by means of a computer. A ramp signal generated from a computer scans the laser wavelength across the absorption line. In addition, a sine wave signal modulates the laser wavelength at a frequency $f = f_0/2$. The DFB laser beam was directed to the erbium-doped fiber amplifier (Connect Laser Technology, Ltd., Model MFAS-L-EY-B-MP) by means of an optical fiber. An opto-isolator (Connect Laser Technology, Ltd., Model A12104132) was utilized to protect the DFB laser against back reflections. The output laser beam from the opto-isolator was directed to a 0.22 mm-diameter light spot by a fiber collimator (OZ optics, Ltd., Model LPC-01), and then passed through the AmR and between the QTF prongs without touching any surfaces. The output from the QTF is connected to a low noise transimpedance amplifier with a feedback resistor of 10 MΩ and directed to a lock-in amplifier (Stanford Research Systems, Model SR830) for 2*f* detection.[22] The lock-in amplifier was set to a 12 dB/oct filter slope and a time constant $\tau = 300$ ms corresponding to a detection bandwidth of $\triangle f = 0.833$ Hz.

Performances of this sensor spectrophone were optimized by selecting $CO_2$ as the target gas from a certified gas mixture of 5% $CO_2$ in $N_2$ at atmospheric pressure and room temperature. The selected $CO_2$ target line is located at 6325.1374 $cm^{-1}$ with a line intensity of $1.155 \times 10^{-23}$ cm $mol^{-1}$.[23] The output power of the erbium-doped fiber amplifier was ~1500 mW. The optimum AmR vertical position was identified by using a pair of tubes whose inner diameter (*r*) and length (*l*) were 1.3 mm and 12 mm, respectively. The gaps between the QTF and the tubes were 30 μm. The highest signal amplitude was achieved when the distance *y* between the tube center and top surface of the QTF tines is ~1.2 mm, as shown in Fig. 3(a).

Since variations in *l* as small as 0.2 mm have a significant impact on the spectrophone properties, six AmRs with different *l* were tested for further improving the detection sensitivity.[7] Serebryakov *et al.* confirmed that the optimum length of the tube is between $\lambda_s/4$ and $\lambda_s/2$, where $\lambda_s$ is the sound wavelength ($\lambda_s \sim 47$ mm for $f_0 \sim 7205$ Hz).[24]

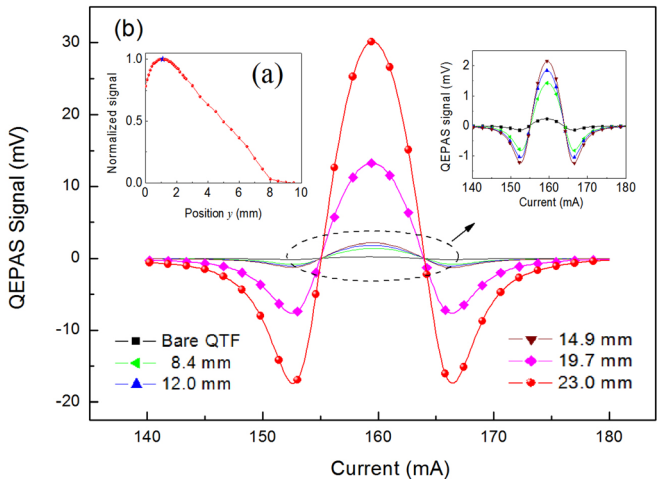


FIG. 3. (a) The normalized signal amplitude as a function of the AmR (r = 1.3 mm and l = 12 mm) vertical axial position between the tube center and top surface of the custom QTF tines. (b) Second-harmonic QEPAS signal for the sensor with five different AmRs. The signal of the fiber-amplifier-enhanced QEPAS sensor with a bare custom QTF was also shown. All spectra were acquired at atmospheric pressure ($P_0$ = 760 Torr) and room temperature (T = 297.2 K).

The length of the AmRs were in the range of 0 mm (bare QTF) to $\lambda_s/2 \sim 23$ mm. The second-harmonic QEPAS signals from the sensor with six different AmRs were detected, as shown in Fig. 3. This studies revealed that the optimized length of the tube ($r = 1.3$ mm) for a custom QTF was $l = 23$ mm ($\sim\lambda_s/2$), and that the use of an optimized AmR can improve the signal-to-noise ratio (SNR) by a factor of up to ~40, compared to the case of a bare custom QTF. Longer tubes have not been tested due to high difficulty in alignment of the laser beam through longer AmR tubes and its focalization between the QTF prongs without hitting both them.

The background noise, $Q$-factor and SNR as a function of $l$ is plotted in Fig. 4. The $Q$-factor gradually decreases with $l$. This implies that the acoustic coupling between the QTF and AmR is more efficient for longer tube length and the high-$Q$ QTF transfer energy occurs primarily via coupling to the low-$Q$ AmR oscillator.[25,26] Therefore, the SNR increases with $l$ to its maximum value of $l = 23$ mm. The observed gradual increase of the background noise is mainly due to the increasing difficulty in aligning the high power laser beam passing through the AmR and the QTF without optical contact. In addition, with the more efficient coupling between the quadrupole-like QTF and the dipole-like AmR, the system becomes susceptible to environmental acoustic noise, due to the lower resonant frequency and the weaker immunity of the dipole-like AmR to external acoustic noise compared with the quadrupole-like QTF system.

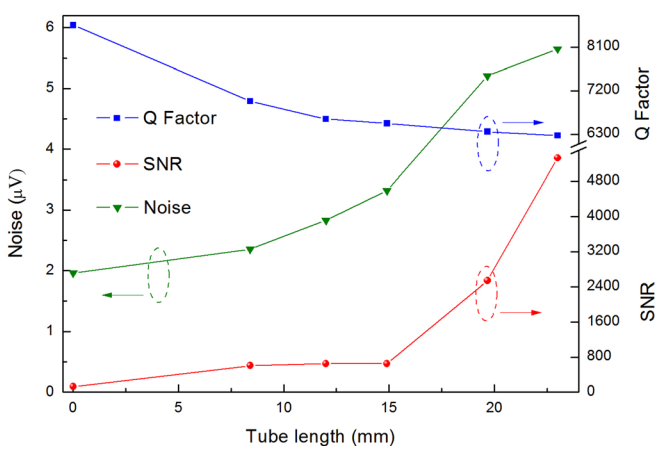


FIG. 4. $Q$-factor (blue squares), SNR (red dotted symbols), and background noise (green triangles) of the fiber amplified enhanced QEPAS sensor as a function of AmR tube length.

As a second step, the detection sensitivity of an optimized fiber-amplifier-enhanced sensor for $H_2S$ detection was investigated. A $H_2S$ absorption line at 6320.6 $cm^{-1}$ with a line intensity of $1.1 \times 10^{-22}$ cm $mol^{-1}$ was selected as the target line.[23] The $2f$ signal measured for a certified 50 ppm $H_2S$:$N_2$ mixture with a current modulation depth of 18 mA at room temperature is shown in Fig. 5. The measurements were carried out at atmospheric pressure for convenience, since the signal amplitude at atmospheric pressure is only ~8% lower than that at the optimal pressure of 400 Torr.[12] The selected target line merges with weaker sidebands located at 6320.5 $cm^{-1}$ and 6320.9 $cm^{-1}$, which results in slight asymmetry of the $2f$ QEPAS signal. A 1 $\sigma$ minimum detectable concentration limit of 890 ppb was obtained for a 1 s data acquisition time and 1520 mW laser power, which is similar to that obtained by a fiber-amplifier-enhanced QEPAS sensor with a standard QTF (730 ppb),[12] but with a significantly simpler sensor configuration. The corresponding normalized noise equivalent absorption (NNEA) coefficient for $H_2S$ is $1.29 \times 10^{-8}$ W $cm^{-1}/\sqrt{Hz}$. A previous research showed that water vapor has an influence on $H_2S$ signal by acting as a promoter of vibrational-translational relaxation processes.[27,28] In the near-infrared region, the sensitivity can be improved by 10% when in the presence of few percent of water vapor concentration,[28] leading to the necessity of a sensor calibration if monitoring a humid $H_2S$ sample.

In order to evaluate the long-term stability of the fiber-amplifier-enhanced QEPAS sensor, we performed an Allan–Werle deviation analysis,[29] measuring and averaging the

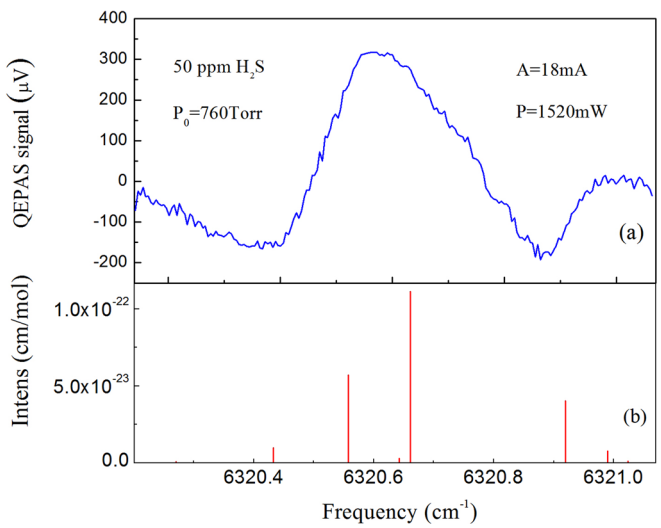


FIG. 5. (a) Spectral scan of 50 ppm $H_2S$ in $N_2$ at atmospheric pressure and room temperature, acquired with a modulation depth of 18 mA and a 1s integration time. (b) Line strengths of the main $H_2S$ transitions, as reported in the HITRAN database,[23] falling in the spectral range corresponding to the frequency scan of Fig. 5(a).

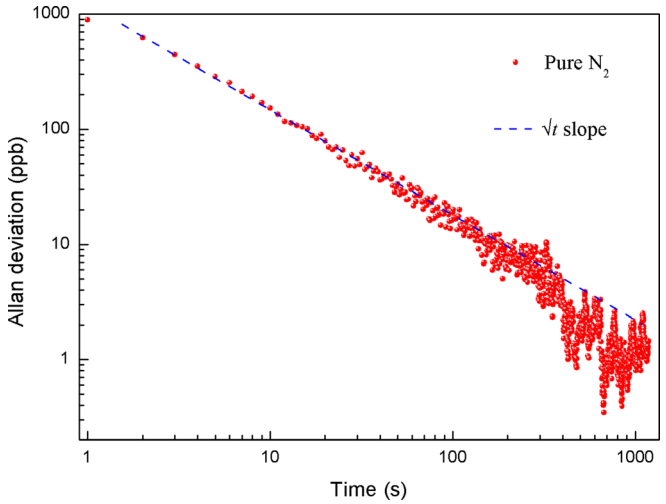


FIG. 6. Allan–Werle deviation as a function of the data averaging period. Solid circles trace: laser frequency was locked to a $H_2S$ absorption line at 6320.6 $cm^{-1}$, the data acquisition time was 1 s. Dashed line represents the $1/\sqrt{t}$ slope.

QEPAS signal at zero $H_2S$ concentration (pure $N_2$), as shown in Fig. 6. The Allan–Werle deviation for all time sequences closely follows a $1/\sqrt{t}$ dependence over the entire duration of the measurement series, which indicates that thermal noise of the QTF remains the dominant noise source and the sensor allows data averaging without base line or sensitivity drift on a more than 1000 s time scale.

In conclusion, a fiber-amplifier-enhanced QEPAS sensor with a custom QTF was developed for $H_2S$ detection. The larger spatial separation between the QTF prongs allows the QEPAS based sensors benefit from the power boosted by an erbium-doped fiber amplifier, while preventing the prongs and AmR to be illuminated by stray light, thus facilitating the assembly of the spectrophone and improving the long-term stability of the sensor. Our results show that the detection sensitivity of the sensor was improved by a factor of ~40, when implementing and optimizing an "on-beam" AmR configuration. Further improvement of the detection sensitivity can be expected by operating at low gas pressure and by further optimizing the AmR geometrical parameters, such as inner and outer tube diameters and QTF-tube spacing.

Lei Dong acknowledges support by National Natural Science Foundation of China (Grant Nos. 61575113 and 61275213), the Shanxi Natural Science Foundation (2013021004-1), and the Shanxi Scholarship Council of China (2013-011, 2013-01). Frank Tittel acknowledges support by the National Science Foundation (NSF) ERC MIRTHE award and the Robert Welch Foundation (Grant No. C-0586). The authors from Dipartimento Interateneo di Fisica di Bari acknowledge financial support from two Italian Research Projects: PON02 00675 and PON02 00576.

[1]Y. Ma, X. Yu, G. Yu, X. Li, J. Zhang, D. Chen, R. Sun, and F. K. Tittel, Appl. Phys. Lett. **107**, 021106 (2015).
[2]N. Petra, J. Zweck, A. A. Kosterev, S. E. Minkoff, and D. Thomazy, Appl. Phys. B **94**, 673 (2009).
[3]Y. Cao, W. Jin, L. Ho, and Z. Liu, Opt. Lett. **37**, 214 (2012).
[4]L. Dong, J. Wright, B. Peters, B. A. Ferguson, F. K. Tittel, and S. McWhorter, Appl. Phys. B **107**, 459 (2012).
[5]A. A. Kosterev, Y. A. Bakhirkin, R. F. Curl, and F. K. Tittel, Opt. Lett. **27**, 1902 (2002).
[6]P. Patimisco, G. Scamarcio, F. K. Tittel, and V. Spagnolo, Sensors **14**, 6165 (2014).
[7]L. Dong, A. A. Kosterev, D. Thomazy, and F. K. Tittel, Appl. Phys. B **100**, 627 (2010).
[8]K. Liu, X. Guo, H. Yi, W. Chen, W. Zhang, and X. Gao, Opt. Lett. **34**, 1594 (2009).
[9]H. Yi, K. Liu, W. Chen, T. Tan, L. Wang, and X. Gao, Opt. Lett. **36**, 481 (2011).
[10]V. Spagnolo, A. A. Kosterev, L. Dong, R. Lewicki, and F. K. Tittel, Appl. Phys. B **100**, 125 (2010).
[11]L. Dong, V. Spagnolo, R. Lewicki, and F. K. Tittel, Opt. Express **19**, 24037 (2011).
[12]H. Wu, L. Dong, H. Zheng, X. Liu, X. Ying, W. Ma, L. Zhang, W. Yin, S. Jia, and F. K. Tittel, Sens. Actuators, B: Chem. **221**, 666 (2015).
[13]S. Borri, P. Patimisco, I. Galli, D. Mazzotti, G. Giusfredi, N. Akikusa, M. Yamanishi, G. Scamarcio, P. D. Natale, and V. Spagnolo, Appl. Phys. Lett. **104**, 91114 (2014).
[14]M. E. Webber, M. Pushkarsky, and C. K. N. Patel, Appl. Opt. **42**, 2119 (2003).
[15]Y. Cao, W. Jin, and L. Ho, Sens. Actuators. B: Chem **174**, 24 (2012).
[16]L. Dong, H. Wu, H. Zheng, Y. Liu, X. Liu, W. Jiang, L. Zhang, W. Ma, W. Ren, W. Yin, S. Jia, and F. K. Tittel, Opt. Lett. **39**, 2479 (2014).
[17]P. W. France, *Optical Fiber Lasers and Amplifiers* (CRC Press, Boca Raton, FL, 1991).
[18]P. M. Becker, A. A. Olsson, and J. R. Simpson, *Erbium-Doped Fiber Amplifiers: Fundamentals and Technology* (Academic Press, Manhattan, New York, 1999).
[19]P. Patimisco, A. Sampaolo, L. Dong, M. Giglio, G. Scamarcio, F. K. Tittel, and V. Spagnolo, "Analysis of the electro-elastic properties of custom quartz tuning forks for optoacoustic gas sensing and scanning microscope applications," Sens. Actuator, B: Chem. (submitted).
[20]S. Borri, P. Patimisco, A. Sampaolo, H. E. Beere, D. A. Ritchie, M. S. Vitiello, G. Scamarcio, and V. Spagnolo, Appl. Phys. Lett. **103**, 021105 (2013).
[21]V. Spagnolo, P. Patimisco, S. Borri, A. Sampaolo, G. Scamarcio, M. S. Vitiello, H. E. Beere, and D. A. Ritchie, in *Quantum Sensing and Nanophotonic Devices XI*, edited by M. Razeghi, E. Tournié, and G. J. Brown (San Francisco, California, 2013), p. 899320.
[22]H. Yi, R. Maamary, X. Gao, M. W. Sigrist, E. Fertein, and W. Chen, Appl. Phys. Lett. **106**, 101109 (2015).
[23]See http://www.hitran.com for HITRAN database.
[24]D. V. Serebryakov, I. V. Morozov, A. A. Kosterev, and V. S. Letokhov, Quantum Electron. **40**, 167 (2010).
[25]R. D. Grober, J. Acimovic, J. Schuck, D. Hessman, P. J. Kindlemann, J. Hespanha, and A. S. Morse, Rev. Sci. Instrum. **71**, 2776 (2000).
[26]H. Wu, L. Dong, W. Ren, W. Yin, W. Ma, L. Zhang, S. Jia, and F. K. Tittel, Sens. Actuators, B: Chem. **206**, 364 (2015).
[27]S. Viciani, M. S. de Cumis, S. Borri, P. Patimisco, A. Sampaolo, G. Scamarcio, P. De Natale, F. D'Amato, and V. Spagnolo, Appl. Phys. B **119**, 21 (2015).
[28]A. A. Kosterev, L. Dong, D. Thomazy, F. K. Tittel, and S. Overby, Appl. Phys. B **101**, 649 (2010).
[29]P. Werle, Appl. Phys. B **102**, 313 (2011).